Earth and Climate Physics Project 7 - Timing of Glaciations

Carl Askehave & Lea Bauer

3rd of November 2023

1 Introduction

In 1998 french researcher Didier Paillard released a paper in which he seeks to explain the glacial-interglacial cycles in the Earth's climate over the past million years, and specifically probe a mechanism for the appearance of a 100 kyr signal in the isotope records from marine and ice cores and a resolution to the so called stage 11 problem, where an interglacial stage occurs despite rather low insolation maxima. Using a numerical model, he attempts to replicate the δ^{18}O signatures in data from several geological oxygen isotope records.

In this report we seek to build a replica of Paillard's model to understand what he did and how to implement it ourselves. We will showcase the mathematics involved, but will not include any explicit code. After implementing the model, we run it on two different sets of input data, and test it against paleoclimatic data from ice cores and marine cores. Paillard's model is subject to some assumptions about the nature of the climate system, we will examine and discuss these, in order to better evaluate our findings. Afterwards we will examine how stable our model is to variations in its parameters. Lastly we will put forth our results and give an interpretation of these.

2 Data

Fundamentally, the model is interested in the total ice volume on Earth, and thus the energy-content of the Earth-system. Since nearly all of that energy comes from solar insolation, we use this as input for the model.

To evaluate whether the model is effective at explaining the dynamics of the glacial-interglacial cycles we compare the model results to several isotope records from marine and ice cores.

2.1 Astronomical Data

The insolation data that we will use as input for our model is obtained through astronomical calculations, and we will be using two such data sets, which we will refer to as the Laskar[7] and Berger[2] sets respectively. Both data sets include several of the Earth's orbital parameters, including *eccentricity*, *precession* and *obliquity* and then the *insolation*. Both data sets are numerical calculations of the same thing, and thus should be

expected to depict the same situation, but as can be seen in Figure (1), they do differ slightly.

Input Normalization

Before inputting the insolation data into the model, we normalize it to unity variance and zero mean. This is done by subtracting the mean from the data and dividing by the standard deviation like so:

$$\hat{X} = \frac{X - \mu}{\sigma} \qquad \text{where} \quad \mu = \frac{\sum_i^N x_i}{N} \quad \text{and} \quad \sigma = \sqrt{\frac{\sum_i^N (x_i - \mu)^2}{N}}$$

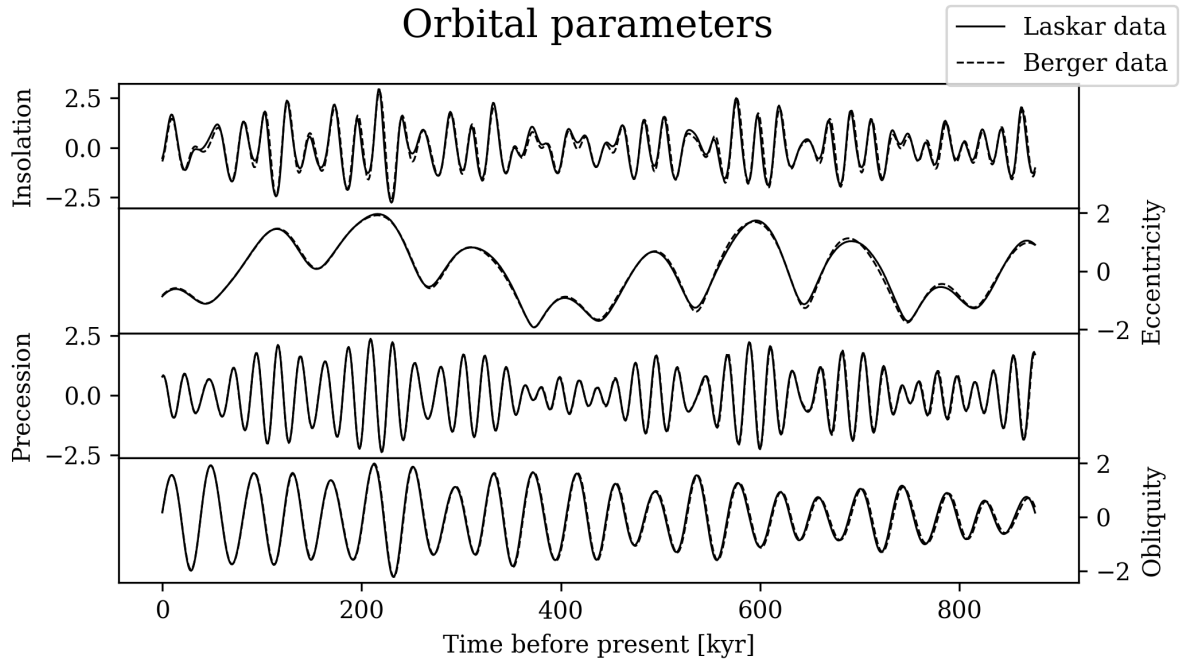

Figure 1: *Orbital parameters from the two different data sets. The Laskar set is depicted with the opaque line and the Berger set with the dashed one. It is seen that although very similar, they do differ slightly, especially in the insolation.*

2.2 Isotope Data

To evaluate the output of our model, we'll compare to paleoclimatic data from an ice core and marine cores in the form of δ^{18}O-records. The marine core data set that we have used is the combined data from 57 different global δ^{18}O-records called the LR04 δ^{18}O-set as presented in[8] and it can be seen in Figure (2). The ice core data set that we have used is a δ^{18}O-record obtained from the EPICA DomeC site in Antarctica called the EDC set as presented in[6] and it can be seen in Figure (3). It should be noted that, since the records from ice cores (EDC) inform of the past surface temperature at the site, and records from $CaCO_3$ from marine cores (LR04) inform of past volume of land ice, the data sets are expected to be different. This is also what you see, when you compare Figure (2) and (3).

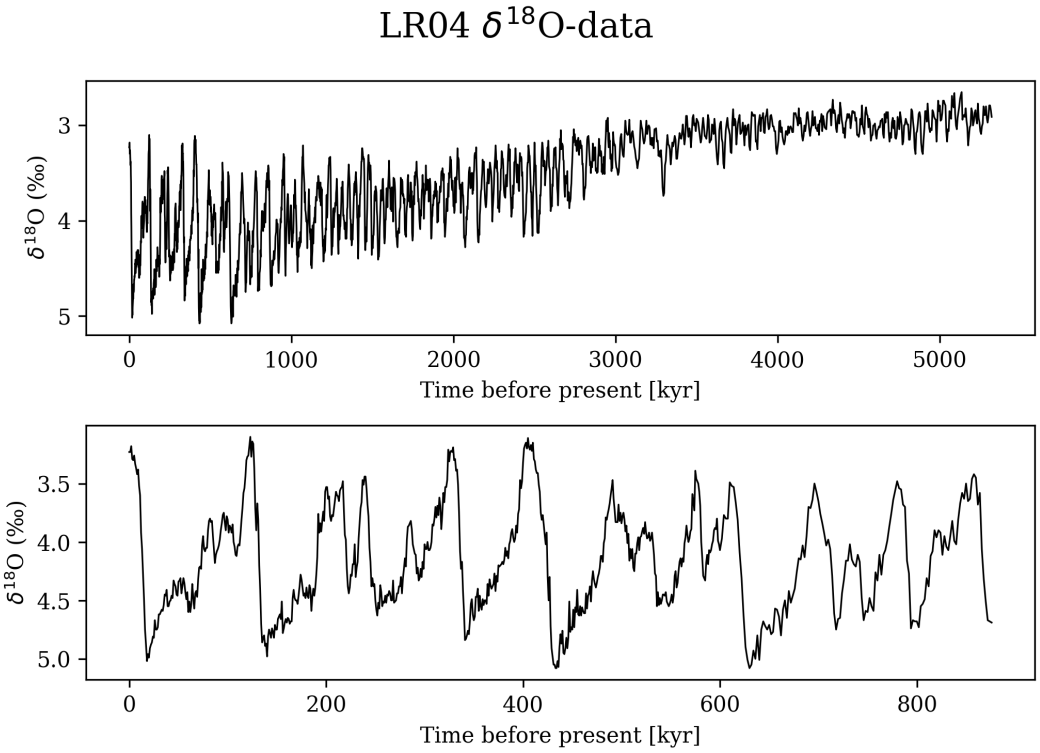

Figure 2: *The LR04 data set containing stacked $\delta^{18}O$-data from 57 global sources going back a maximum of 5.3 Myr. Note the y-axis is flipped so that an upward change in the graph corresponds to an increase in temperature. It is seen on the top plot, that the temperature has been steadily decreasing during the last 5 Myr, and the variation in temperature between periods of high and and low temperature has increased. On the bottom plot the same data is shown but only from 876 kyrs in the past.*

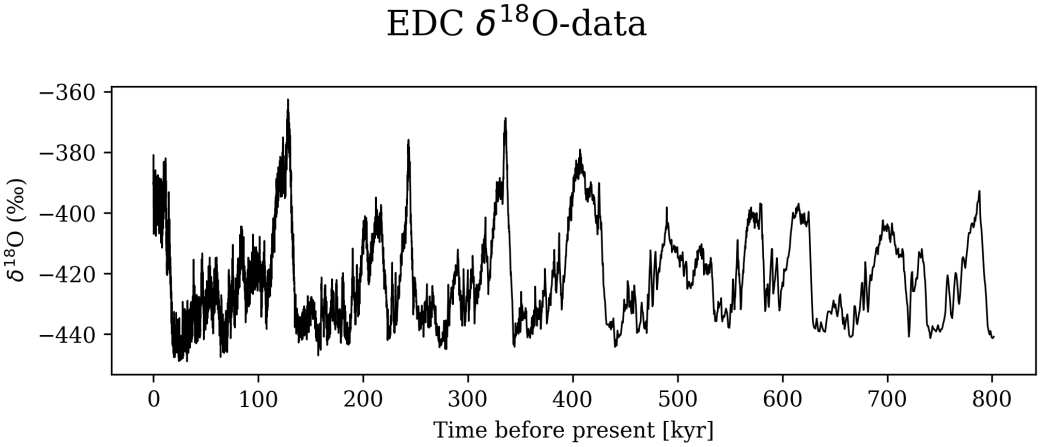

Figure 3: *The EDC $\delta^{18}O$-data set obtained from an ice core at the EPICA DomeC site in Antarctica. This data set only goes back to 800 kyrs before the present, and it can be seen that, although the peaks line up with the LR04 records, the general profile of this data differs a significant amount from that of the marine cores.*

3 Methods: Modelling the Glacial-Interglacial Cycles

3.1 The Climate State Model

In his paper, Paillard first introduces the model which he calls model 1, but we will refer to as the climate state model. The defining feature of this model, is the assumption that the climate system can be in one of three states at a time, namely the interglacial state **i**, the mild glacial state **g** and the full glacial state **G**. Which state the model is in at a given time is determined by the *insolation* at a given time $i(t)$ (taken from the astronomical data sets), the *time since the last state change* t_c, the ice sheet growth time t_g, and the four insolation parameters i_0, i_1, i_2 and i_3, which are set to fit the model to the data.

More precisely the state transitions occur in the following circumstances:

$$\begin{aligned}
\mathbf{i} \to \mathbf{g}: &\quad \text{If} \quad i < i_0 \\
\mathbf{g} \to \mathbf{G}: &\quad \text{If} \quad t_c > t_g, \quad i < i_2, \quad i_{\mathrm{p}} \geq i_2 \quad \text{and} \quad i_{\mathrm{max,p}} < i_3 \\
\mathbf{G} \to \mathbf{i}: &\quad \text{If} \quad i > i_1
\end{aligned}$$

Here i_{p} is the previous insolation before crossing i_2 and $i_{\mathrm{max,p}}$ is the previous insolation maximum. Notice that the transitions $\mathbf{G} \to \mathbf{g}$, $\mathbf{i} \to \mathbf{G}$ and $\mathbf{g} \to \mathbf{i}$ are forbidden by assumption. More about that later.

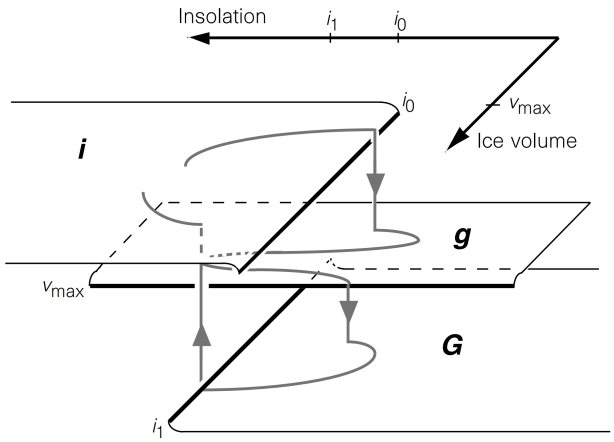

Figure 4: *Visualization of the different states and the transitions between them as influenced by the insolation i and the ice volume v.*

3.2 The Ice Volume Model

The advancement of the simple climate state model is the model that Paillard calls model 2, but which we will refer to as the ice volume model. The key feature about this model is that its primary output is a continuous calculation of the total ice volume on earth as a function of time depending on the insolation, and that it uses the results of this calculation to determine the climate state changes. So key parts of the climates state model is still included in this model.

The change in ice sheet volume is described by the differential equation

$$\frac{dv}{dt} = \frac{v_R - v(t)}{\tau_R} - \frac{F}{\tau_F}, \tag{1}$$

where $v(t)$ is the ice volume at a given time t, R is the current climate state ($R = \mathbf{i}, \mathbf{g}, \mathbf{G}$), v_R are the different ice volume thresholds depending on the current state, F is the forcing and τ_R and τ_F are time constants. The v_R parameters are set accordingly $v_g = v_G = 1, v_i = 0$, and the parameter $v_{\max} = 1$ is used in the state transitions, which now occur in the following circumstances:

$$\begin{aligned} \mathbf{i} \to \mathbf{g}: &\quad \text{If} \quad i < i_0 \\ \mathbf{g} \to \mathbf{G}: &\quad \text{If} \quad v > v_{\max} \\ \mathbf{G} \to \mathbf{i}: &\quad \text{If} \quad i > i_1 \end{aligned}$$

Due to the lower sensitivity to the insolation of the ice volume during cold periods[9], we truncate the insolation forcing F with a truncation function

$$f(x) = \frac{1}{2}\left(x + \sqrt{4a^2 + x^2}\right) \tag{2}$$

The amount of truncation depends on the parameter a, where $a = 0$ results in maximal truncation and $a = \infty$ results in no truncation (after normalization). Paillard chooses $a = 1$, which makes the in minima less negative and the maxima a bit more positive.

3.3 Expanded Ice Volume Model and Spectral Analysis

The model which Paillard calls model 3 we call the expanded ice volume model, as the code is unchanged, but a linear increase is added to both the insolation forcing and the ice volume threshold $v_{\max}$. To examine whether this model is a good explanation of the 100 kyr signal, we perform a spectral analysis on the δ^{18}O-data and the results from this expanded model to probe the dominant frequency signals in each and compare. We do this by doing a series of Fourier transformations with time windows of 400 kyrs, with around 60 kyrs overlap between them. This results in a spectrogram displaying which frequencies appear in the signal as a function for time. It is important that we keep the windows an appropriate size relative to the frequencies we're probing, as the Fourier analysis cannot pick up a 100 kyr frequency in a window that's smaller than that, and even when the window size is on the order of 100 kyr there is a great uncertainty in the specific frequency values of frequencies of similar size. We also don't want to choose a window size too large, because although we can know the frequency values to great precision there's a great uncertainty in exactly when the frequencies occur in the signal.

4 Assumptions

4.1 The Climate State Model

The climate state model is inspired by the simplified ocean model, where the ocean is divided into "boxes" and it is assumed that the water in these boxes is well-mixed within each box, and differ in densities. In 1961, Stommel showed that the thermohaline circulation between such boxes caused by the density differences can have several steady states.[11] In conjuction with the later work by Rahmstorf[10], who showed that thermohaline circulation and the steady states are dependent on the changing of the freshwater input, the general understanding is that these steady states exist between reservoirs with fluids of different densities and properties. We assume that the same applies to our case, where

the reservoirs are the atmosphere, ocean and ice sheets. We call the steady states **i**, **g** and **G**. These steady states and the state-dependent thresholds between them then amount to one of the simplest nonlinear mechanisms with which to model the 100-kyr climate signal found in the paleoclimatic data. This signal is not linearly related to the insolation forcing.[9] In addition to that, we know that high resolution climate records show that abrupt transitions are very common, which also suggests a model of this character with thresholds between different steady states.[1,3]

In the model we assume that the transitions go in a particular order, and that the transitions $\mathbf{G} \to \mathbf{g}$, $\mathbf{i} \to \mathbf{G}$ and $\mathbf{g} \to \mathbf{i}$ are forbidden. The $\mathbf{i} \to \mathbf{G}$-transitions are forbidden, because then there would be no time for the ice sheet to grow, and have an impact on the climate. The $\mathbf{g} \to \mathbf{i}$-transition is forbidden, because as the ice sheet is growing, and the required insolation to not only negate the growing, but also melt the ice is assumed to be out of reach.[9] The role of the states is to emulate the processes observed in the data, which is cycles of rapid heating (**i**) and less rapid cooling (**g**) and a short stagnation period (**G**). Thus it doesn't make sense for the model to go from the **G** state back to the **g** state.

In the climate state model there are four parameters that have to be chosen. The minimal duration of a **g** state is chosen in the paper to be $t_g = 33$ kyr. To justify this, assumption one has to look at the δ^{18}O records we compare our data with. Here we can see that the shortest glaciation at around 780 kyr BP has a build-up duration of around 33 kyr. We don't want to choose this value too much bigger or lower, because then the model will go into glaciations too early or too late. This includes others factors that may contribute to the fact, that we have no shorter glaciations than 30 kyr.

In addition to the time threshold, we choose the insolation thresholds i_0, i_1, i_2 and i_3, because we know that the total volume of land ice is dependent on the insolation and a threshold system is the simplest non-linear mechanism to model the states with. For the insolation thresholds Paillard chooses the values $i_0 = -0.75$, $i_1 = i_2 = 0$ and $i_3 = 1$. One reason for choosing $i_1 = i_2$ is that it is the most plausible to assume that the threshold at which we enter a **G**-state and the threshold at which we leave **G** again are the same. The values of the parameters i_0 and i_3 reflect that the deviation of the normalized insolation from zero has to be greater in the positive direction to invoke a $\mathbf{g} \to \mathbf{G}$-transition, than it has to be in the negative direction to invoke a $\mathbf{i} \to \mathbf{g}$. This means that the model is more sensitive to a dip in insolation, than to an increase.

4.2 The Ice Volume Model

The climate state model accounts for the growth of the ice only by requiring the growth time t_g to pass before entering a glacial **G** period, but this is a lackluster approximation. Thus to capture and investigate the assumption that the glacial–interglacial cycles are closely related to the build-up and melting of the Laurentide and Fennoscandian ice sheets at high northern latitudes[9] we now assume that the ice volume can be described by the differential equation (1) and completely governs the $\mathbf{g} \to \mathbf{G}$-transitions. This assumption is backed by[4,5] where arguments are made for strong correlations between the volume of the Laurentide and Fennoscandian ice sheets and glacial-interglacial cycles with around 23 kyr, 41 kyr and 100 kyr periods.

4.3 Expansion of Ice Volume Model with General Cooling

In the third model we assume a general cooling over time, which is why the ice volume threshold $v_{\max}$ increases linearly over time. Additionally we try to include the effects of slight tectonic changes 2000 kyr before present which cause a decreases the amount of atmospheric CO_2 concentration.[9] This affects our model in two ways. It contributes to the increase in the ice volume threshold $v_{\max}$, and also to a slight increase in the insolation. The mechanism which causes this effect is that when the concentration of CO_2 is lower, certain locations would become colder for a given insolation. This also means that ice sheets can grow up until higher insolation values. This equates to artificially adding an increase to the insolation. Here we assume a small increase of 3 $\mathrm{W\,m^{-2}\,Myr^{-1}}$ in the insolation.

5 Results

5.1 The Climate State Model

Running our climate state model on the two astronomical data sets we get the following result.

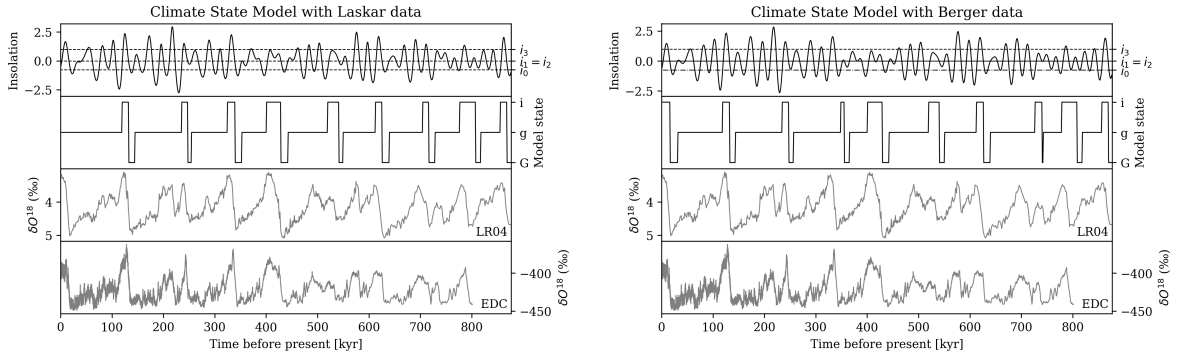

Figure 5: *Plot of the climate state model run on the Laskar data (left) and the Berger data (right).*

We see that the Laskar results has a high correlation with data but has a rather large discrepancy in the latest 10 kyr period, which is gone in the Berger results. If we change the value for i_1 and i_2 to $i_1 = i_2 = -0.08$ the discrepancy is now gone in both cases.

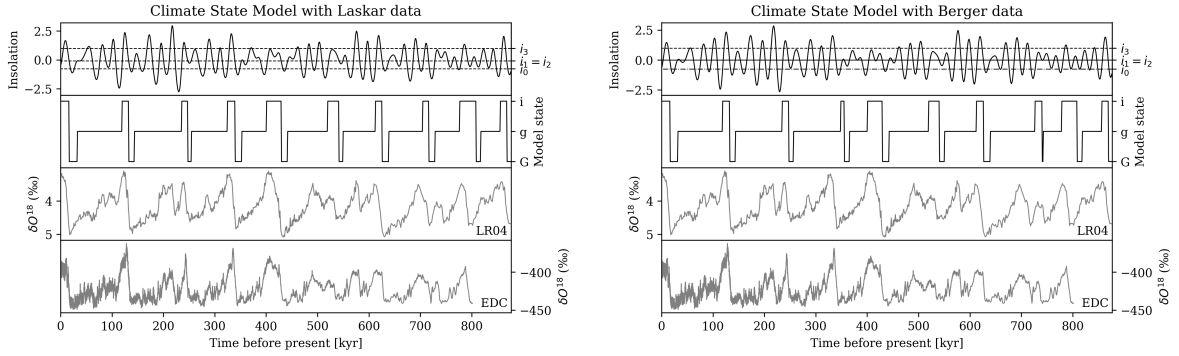

Figure 6: *Plot of the climate state model run on the Laskar data with* $i_1 = i_2 = -0.08$ *(left) and the Berger data with original parameters (right).*

Comparing the tweaked Laskar data model and the Berger model it is seen that the Laskar model has a higher correlation with the peaks in our δ^{18}O records. At 340 kyrs BP the peak in δ^{18}O in the two records match up exactly with the **i** state. In the Berger model this isn't the case. There is also an improvement in matching up the peaks in δ^{18}O with the i state at 410 kyrs BP and at 700 kyrs BP.

To see how robust the model is when running on the Laskar data, we will now try varying the parameters for this case. When varying the time constant t_g in the range 22 kyrs $\leq t_g \leq$ 45 kyrs we get no significant deviation in our results. With $-0.85 \leq i_0 \leq -0.58$ the model here is similarly unchanged. A change in i_1 doesn't result in a significant change for -0.08 $\leq i_1 \leq$ 0.27. For i_2 the range is $-0.07 \leq i_2 \leq 0$, which is a much smaller range than Palliard got. For i_3 the range is $0.93 \leq i_3 \leq 1.05$. This range is comparable to Paillards. The changing of the parameters yield similar results for the Berger data. Even starting in the wrong state, the model recovers after about 200 kyrs, when the starting state is **g** instead of **i**. For a starting state of **G** instead of **i** the model recovers even faster after less than 20 kyrs. This is also very similar to Paillards observations. Additionally, except for the peak at 600 kyrs BP every **i** state matches up with a peak in the LR04 record. From 0 to 400 kyrs BP this also fits with the EDC records, but then the peaks in the EDC records get less defined and don't match up. This is the case for both data sets.

5.2 The Ice Volume Model

The two different data sets have the same amounts of periods in the **i** state ($v_R = 0$). As was also apparent in the climate state model, the model results when run on the Laskar data have a discrepancy with data in the last 100 kyrs, which is gone when run on the Berger data. Otherwise the minima and maxima in the ice volume have a high correlation with the minima and maxima in the δ^{18}O-records when run on either insolation data sets, although the profile of the ice volume has a stronger resemblance to that of the marine sediment data (LR04) than to the ice core data (EDC).

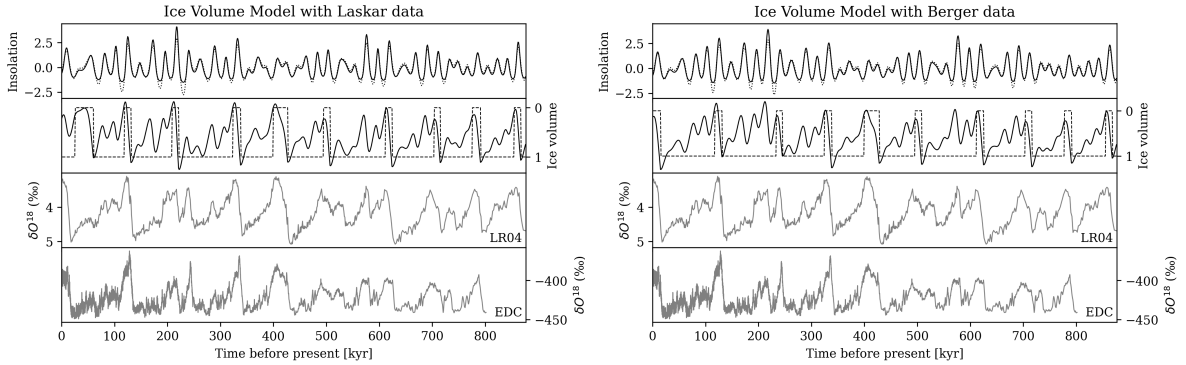

Figure 7: *Plot of the ice volume model run on the Laskar data (left) and Berger data (right). Again we see the discrepancy within the last 100 kyr in the Laskar results, but not in the Berger results.*

Examining again the resilience of the model by varying the parameters, we observe no significant changes for 23 kyrs $\leq \tau_F \leq$ 28 kyrs, 5 kyrs $\leq \tau_i \leq$ 14, 48 kyrs $\leq \tau_g \leq$ 53 kyrs, $5 \leq \tau_G \leq \infty$ kyrs, $0.84 \leq a \leq 1.49$. If we change the starting state, the model is again

divergent for the original first two **i** states, as they get absorbed into one, but returns to correlate with data after this point.

We can also see that the **i** states (i.e. the warmest states with the least ice) don't necessarily occur after high insolation maxima. This can be seen at 400 kyrs BP. Here the insolation maxima are pretty low in comparison to other maxima, but in spite of this an interglacial occurs here, which is in high correlation with the data.

As can be seen in the following graph, changing the mild interglacial time constant $\tau_g = 54$ kyrs instead of 50 kyrs, the discrepancy at 50 kyrs BP disappears.

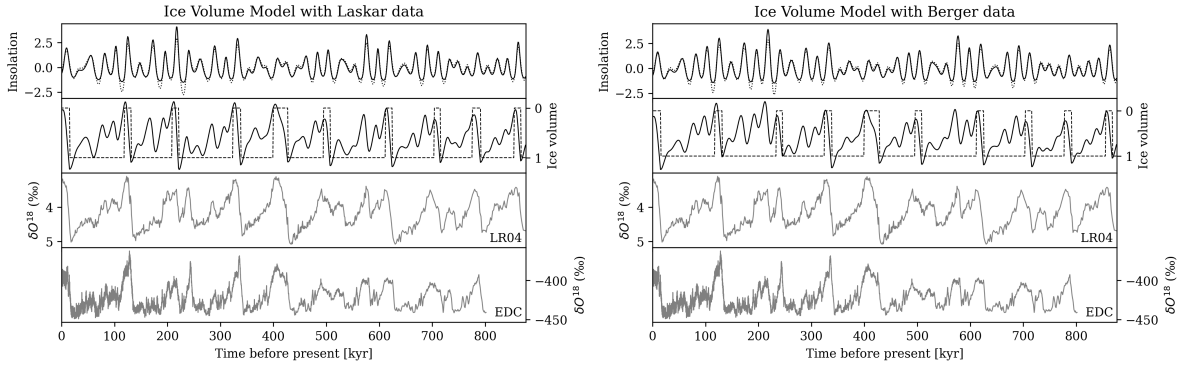

Figure 8: *Plot of the ice volume model run on the Laskar data with changed parameter $\tau_g = 54$ kyrs (left) and the Berger data with unchanged parameter $\tau_g = 50$ kyrs (right).*

The rest of the results except for the point at 50 kyrs BP is virtually unchanged, with only slight changes to the ice volume curve. It is seen in Figure (8) at 180 kyrs BP, at 580 kyrs BP and at 750 kyrs BP that the tweaked model with Laskar data has a higher resemblance to both the marine sediment and the ice core records than the model with Berger data, even exhibiting a sharper peak around 410 kyrs BP.

5.3 Expanded Ice Volume Model and Spectral Analysis

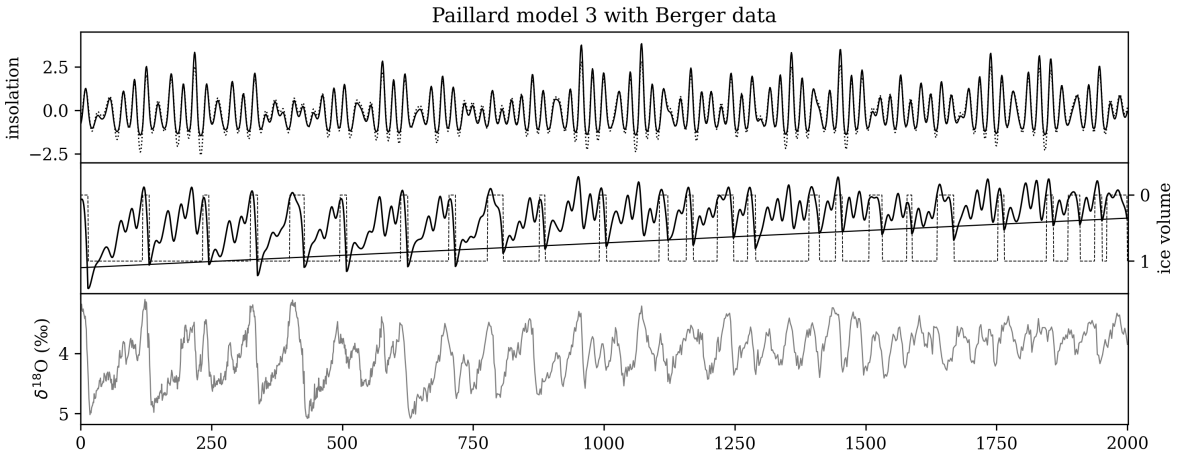

Figure 9: *Plot of the ice volume model over the last 2 Myrs with a linear trend added to $v_{\max}$ (opaque line) and the insolation forcing.*

Although it is apparent from Figure (9) that the relative phases of the glacial cycles from 2 Myrs to 1 Myr cannot be explained by this simple model, other than that, it exhibits similar behaviour to data: starting out with frequent shifts from low to high ice volumes and low amplitude, and then transitioning to less frequent shifts with higher amplitude. It is also apparent from Figure (10) that the model exhibits similar behaviour to the isotope data with a fairly stable 41 kyr signal and a 100 kyr signal appearing and gaining prominence in the last 1000 kyrs before the present.

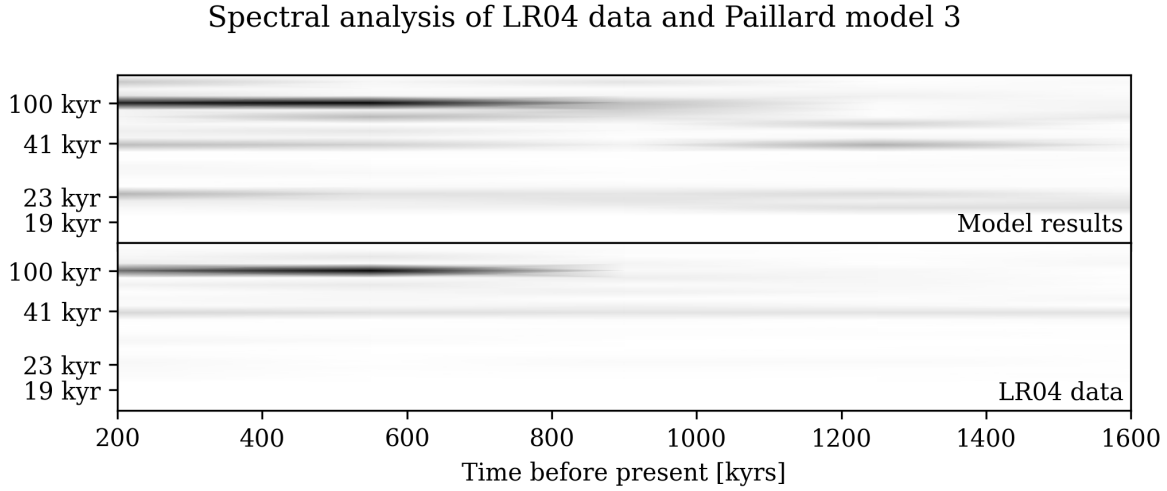

Figure 10: *Spectral analysis of model results (top) and $\delta^{18}O$-data (bottom). We see that the spectral line of the 41 kyr signal is apparent in our model data, and that a 100 kyr signal appears around 800 kyrs before the present.*

Varying parameters to examine model stability, we find the values that produce a system that isn't changed significantly in comparison to the values Paillard chose to be: $0.93 \leq a \leq 1.11$, 26 kyrs $\leq t_F \leq$ 29 kyrs, 4 kyrs $\leq \tau_i \leq$ 12 kyrs, 61 kyrs $\leq \tau_g \leq$ 82 kyrs and 22 kyrs $\leq \tau_G \leq \infty$ kyrs.

6 Interpretation and Conclusion

First we are going to interpret the results from the climate state model. A reason for the sensitivity of the i_2 parameter could be, because at approximately 350 BP there is a local maximum that is very near zero, so that a change in i_2 directly changes the state at this point. The difference between the Laskar and the Berger data is probably, due to the difference in insolation values and the parameters of the model. One would assume that the model with the Laskar data is better, because it combines more and newer calculations of the insolation, but without retuning the model this can lead to worse results. We see after retuning the model, the model fits the δ^{18}O-data better. As we can see in Figure (6), the rest of the data fits the δ^{18}O records as well and it hasn't changed while tweaking. This results in a better fit for the data in general.

Moving on to the ice volume model, it can be seen that our assumptions of parameter values and state changing criteria and thresholds capture the dynamics well, because of the good fit between the δ^{18}O records and our calculated ice volume. When we try varying the parameters with the Laskar data, we get pretty similar results as Paillard. The model is also very insensitive to changes in τ_G and there is a range for τ_g and τ_i that

are a bit smaller than Paillard, but this small difference can be accredited to the different data sets.

It is surprising that the range for no significant change for τ_i and τ_g is with 10 and 5 kyrs pretty small, whereas for τ_G this is infinity. A possible explanation for this, could be the variations in lengths of the different climate states. The duration of the **g** state is always larger than that of the **i** state. Additionally, the duration of the **i** state is always larger than that of the **g** state. The longer a state lasts the more time the model has available to change, so the ice volume is more sensitive to changes in parameters. For example the **G** state lasts a relatively short time (down to only a couple of kyrs) which is why the time constant τ_G can be varied very much, while still achieving the same results. For the Laskar data the model was tuned again to fit the data with slight changes in τ_g. Here we have better results as well with the Laskar data, which means that the model now makes better predictions.

Interestingly increasing the truncation parameter to $a = 0.83$ fixes the problem with the Laskar data at 50 kyrs BP as well. This makes sense as a decrease in a is an increase in the truncation (see equation (2)). The truncation makes the maxima in the insolation a bit higher and smooths out the minima, so on average the forcing is higher after truncation than before. This increase in forcing leads, according to equation (1), to a smaller growth in the ice volume. Therefore the ice volume doesn't reach the threshold at 50 kyrs BP and the graph looks similar to the Paillard data.

When analyzing the stability of the expanded ice volume model, there aren't many differences to the normal ice volume model. It makes sense for the range of the truncation parameter to be different than before expanding the model, because we also changed the other time threshold parameters. Similarly to the normal ice volume model, τ_G has a big range of possible values without changing the plot. τ_i and τ_g have similar ranges than in the normal ice volume model. Looking at the plot from 1000 kyrs BP to 2000 kyrs BP, it can be seen that the plotted ice volume matches up pretty good with the δ^{18}O records in terms of amplitude, but not in terms of the phase. This shows that a more fleshed out version of the model is needed to account for the changes in ice volume over this time. Comparing the model results with marine sediment data (LR04) and the ice core data (EDC), it is clear that our ice volume profile generally fits the LR04 data fits much better. This is probably because marine sediment data informs of the past volume of land ice and ice core data informs about the surface temperature at that time. Therefore it makes sense that our simulated ice volume fits better with the recorded data corresponding to past volume of land ice. Most importantly our normal and expanded ice volume model both correctly exhibits a big peak at the relatively low insolation maxima around 400 kyrs, thus providing a mechanism for explaining the stage-11-problem. I addition, the spectral analysis performed on the extended model exhibited an onset of the 100-kyr frequency within an order of magnitude of 100 kyrs. This provides evidence that the slow tectonic activity that induces topographical changes and a reduction in CO_2 at this time might be the cause for the 100 kyr signal onset.

To conclude, we successfully recreated a replica of Paillard's model and managed to adjust the model to a second, more extensive set of data. With this adjusted set of data we managed to replicate the marine sediment data even better than with the data Palliard used. The models successfully describes the "100 kyr problem" as well as the "stage-11-problem".

References

[1] Jess F. Adkins§ et al. "Variability of the North Atlantic thermohaline circulation during the last interglacial period". In: *Nature* 390.6656 (Nov. 1997), pp. 154–156. ISSN: 1476-4687. DOI: 10.1038/36540. URL: https://doi.org/10.1038/36540.

[2] A. Berger and M.F. Loutre. "Insolation values for the climate of the last 10 million years". In: *Quaternary Science Reviews* 10.4 (1991), pp. 297–317. ISSN: 0277-3791. DOI: https://doi.org/10.1016/0277-3791(91)90033-Q. URL: https://www.sciencedirect.com/science/article/pii/027737919190033Q.

[3] W. Dansgaard, J. W. C. White, and S. J. Johnsen. "The abrupt termination of the Younger Dryas climate event". In: *Nature* 339.6225 (June 1989), pp. 532–534. ISSN: 1476-4687. DOI: 10.1038/339532a0. URL: https://doi.org/10.1038/339532a0.

[4] J. Imbrie et al. "On the Structure and Origin of Major Glaciation Cycles 1. Linear Responses to Milankovitch Forcing". In: *Paleoceanography* 7.6 (1992), pp. 701–738. DOI: https://doi.org/10.1029/92PA02253. eprint: https://agupubs.onlinelibrary.wiley.com/doi/pdf/10.1029/92PA02253. URL: https://agupubs.onlinelibrary.wiley.com/doi/abs/10.1029/92PA02253.

[5] J. Imbrie et al. "On the structure and origin of major glaciation cycles 2. The 100,000-year cycle". In: *Paleoceanography* 8.6 (1993), pp. 699–735. DOI: https://doi.org/10.1029/93PA02751. eprint: https://agupubs.onlinelibrary.wiley.com/doi/pdf/10.1029/93PA02751. URL: https://agupubs.onlinelibrary.wiley.com/doi/abs/10.1029/93PA02751.

[6] J. Jouzel et al. "Orbital and Millennial Antarctic Climate Variability over the Past 800,000 Years". In: *Science* 317.5839 (2007), pp. 793–796. DOI: 10.1126/science.1141038. eprint: https://www.science.org/doi/pdf/10.1126/science.1141038. URL: https://www.science.org/doi/abs/10.1126/science.1141038.

[7] Laskar, J. et al. "A long-term numerical solution for the insolation quantities of the Earth". In: *A&A* 428.1 (2004), pp. 261–285. DOI: 10.1051/0004-6361:20041335. URL: http://vo.imcce.fr/insola/earth/online/earth/online/index.php.

[8] Lorraine E. Lisiecki and Maureen E. Raymo. "A Pliocene-Pleistocene stack of 57 globally distributed benthic δ18O records". In: *Paleoceanography* 20.1 (2005). DOI: https://doi.org/10.1029/2004PA001071. eprint: https://agupubs.onlinelibrary.wiley.com/doi/pdf/10.1029/2004PA001071. URL: https://agupubs.onlinelibrary.wiley.com/doi/abs/10.1029/2004PA001071.

[9] Didier Paillard. "The timing of Pleistocene glaciations from a simple multiple-state climate model". In: *Nature* 391.6665 (Jan. 1998), pp. 378–381. ISSN: 1476-4687. DOI: 10.1038/34891. URL: https://doi.org/10.1038/34891.

[10] Stefan Rahmstorf. "Bifurcations of the Atlantic thermohaline circulation in response to changes in the hydrological cycle". In: *Nature* 378.6553 (Nov. 1995), pp. 145–149. ISSN: 1476-4687. DOI: 10.1038/378145a0. URL: https://doi.org/10.1038/378145a0.

[11] HENRY STOMMEL. "Thermohaline Convection with Two Stable Regimes of Flow". In: *Tellus* 13.2 (1961), pp. 224–230. DOI: https://doi.org/10.1111/j.2153-3490.1961.tb00079.x. eprint: https://onlinelibrary.wiley.com/doi/pdf/10.1111/j.2153-3490.1961.tb00079.x. URL: https://onlinelibrary.wiley.com/doi/abs/10.1111/j.2153-3490.1961.tb00079.x.